Magnetic excitations in Ni_3Al at low energies and long wavelengths

N. R. Bernhoeft and G. G. Lonzarich
Cavendish Laboratory, Cambridge CB3 0HE, United Kingdom

P. W. Mitchell
Physics Department, University of Edinburgh, Edinburgh, EH9 3JZ, United Kingdom

D. McK. Paul
Institut Laue-Langevin, F-38042 Grenoble, France
(Received 21 March 1983)

Neutron scattering studies have been carried out on high-quality specimens of Ni_3Al, giving direct experimental evidence on the nature of low-lying magnetic excitations in an ordered weak metallic ferromagnet both below and above the Curie temperature.

Weak ferromagnetism in ordered metals such as $ZrZn_2$ and Ni_3Al, in which the average atomic spin polarization and Curie temperatures are small, has been a subject of experimental and theoretical interest and controversy for many years. In ideally ordered systems the key issues have been the respective roles of collective and single-particle spin-flip excitations in the thermal magnetic properties,[1-4] the effect of collective spin fluctuations on the electronic band structure,[4,5] and the possibility of paramagnon-mediated superconductivity under suitable conditions.[6] Central to all of these problems is the nature of the magnetic excitation spectrum which remains poorly understood.

In this paper we report the first direct study of the magnetic excitation spectrum at low energies and momenta in one of these materials, Ni_3Al, by inelastic neutron scattering. Measurements were carried out in pure and well-ordered stoichiometric samples by means of small-angle and triple-axis spectrometers at the high-flux reactor, Institut Laue-Langevin (ILL), Grenoble, France. Preliminary measurements averaged over energy and scattering angle in less pure specimens have been reported previously.[7]

Samples (which order in the $L1_2$ structure) were prepared by homogenizing a high-purity melt of zone-refined nickel and aluminium having residual resistivity ratios $[\rho(293\ \mathrm{K})/\rho(4.2\ \mathrm{K})]$ in excess of 2000 and then annealing in a high-purity helium atmosphere for up to six days at various temperatures below the melting point. Polycrystalline specimens of optimum dimensions for the individual spectrometers were spark cut from the most homogeneous parts of the prepared ingots. Homogeneity, purity, and structural order were tested by means of resistivity and magnetization measurements, electron-beam microanalysis, x-ray diffraction, and mass spectrometry. The average resistivity ratios of samples used in the small-angle scattering and triple-axis measurements were 40 and 70, respectively. Metallic impurities are estimated to be less than 20 ppm in total with a maximum of 3 ppm Fe and Co; carbon, silicon, and sulphur levels are estimated to be less than 18 ppm in total.

Small-angle scattering measurements were carried out on the multidetector spectrometer D17 at an incident wavelength of 10.2 ± 0.5 Å. The scattering intensity was averaged over the azimuthal angular range $0° \leq \phi \leq 360°$ and analyzed in steps of 0.2° in the polar angular range $1° \lesssim \theta \lesssim 7°$ (θ is the angle between the incident and scattered beams). The uniform relative efficiencies of the annular groups of detector cells used were established by monitoring the scattering from Perspex, and calibration was via a reference vanadium specimen. A calibrated silicon diode in good thermal contact with the sample gave the temperature in the range $2 \lesssim T \lesssim 100$ K to an estimated precision of ± 0.3 K.

Energy- and momentum-resolved studies were made with the triple-axis crystal spectrometer IN12. Since the best specimens which we wished to study are polycrystalline and the average atomic spin polarization is weak, measurements were carried out in the *forward* direction at *small* scattering angles, $0.5° \lesssim \theta \lesssim 2.0°$, giving access to low-energy magnetic excitations for which the thermal population factor is large.

The spectrometer was operated at fixed outgoing energy (normally 2.5 meV) with use of the pyrolytic graphite monochromator and analyzer crystals. A cooled beryllium filter was inserted between the monochromator and sample to attenuate unwanted flux in the incident beam above 5 meV. To reduce the background at small scattering angles in the forward direction an additional collimator was used between the filter and sample, and the analyzer crystal and detector were carefully screened.

Results from the small-angle spectrometer D17, which give the variations of the scattering intensity with temperature and elastic scattering wave vector q (i.e., $2\pi\theta/\lambda$ at incident neutron wavelength λ and small scattering angle θ), are presented in Figs. 1 and 2. For fixed q the scattering intensity exhibits a monotonic rise below T_c, a plateau followed by a peak near $T_c = 41 \pm 1$ K, and a monotonic fall above T_c. Below approximately 30 K the scattering intensity can be reproduced within experimental error by a model cross section based on the existence of conventional, well-defined, spin-wave modes.[9] The calculation of the scattering intensity at fixed angle takes account of the skewed path of integration in energy–wave-vector space required by energy and momentum conservation, the measured calibration constant, and the effect of instrumental resolution. In our analysis the Debye-Waller and form factors are set to unity, the sample is assumed demagnetized, incident beam unpolarized, and the slight temperature dependence of the nuclear scattering ignored. The effective spin-wave stiffness D and energy gap ϵ_g are taken to be adjustable parameters. Values which provide the best fit to the q dependence *and* magnitude of the observed scattering intensity (relative to the 2-K background level) are given in Fig. 2(a). The low-temperature value of D is consistent, within experimental error, with that obtained from an anlaysis of preliminary small-angle scattering measurements carried out at Harwell.[7]

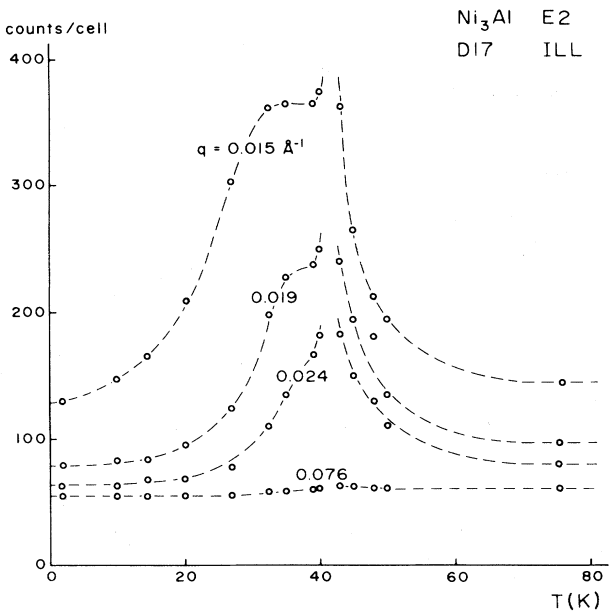

FIG. 1. Temperature dependence of small-angle scattering intensity in the forward direction from stoichiometric Ni_3Al (sample E2, residual resistance ratio $\simeq 40$) averaged over the azimuthal angular range $0° \leq \phi \leq 360°$ for incident neutron wavelength $\lambda = 10.2 \pm 0.5$ Å. q is the magnitude of the *elastic* scattering wave vector in inverse angstroms equal to $2\pi\theta/\lambda$ for a small scattering angle θ. The dashed lines serve to connect data points at fixed scattering angle.

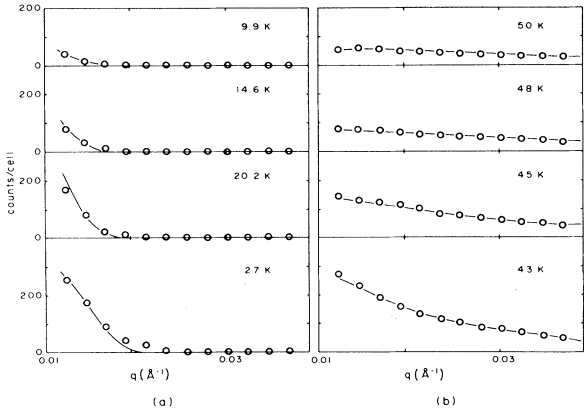

FIG. 2. (a) Wave-vector dependence of small-angle scattering intensity at different temperatures below T_c measured relative to the 2-K background. Solid lines give the absolute intensity calculated in terms of the conventional spin-wave cross section (Ref. 9) convolved with the instrumental resolution function. Vertical calibration [(counts/cell)/ 4×10^6 monitor counts)] was established by monitoring the scattering from a reference vanadium specimen. The fitted values of the spin-wave stiffness D and energy gap ϵ_g [a part of which may be associated with the intrinsic magnetocrystalline anisotropy (Ref. 8)] are found to be $D = 95 \pm 20$, 93 ± 20, 83 ± 20, 78 ± 20 meV Å^2, and $\epsilon_g = 5 \pm 1$, 3.5 ± 0.5, 2.5 ± 0.5, 1.5 ± 0.5 μeV, respectively, for temperatures taken in the order 9.9, 14.6, 20.2, and 27.0 K. (b) The solid lines give the absolute intensity calculated by use of the instrumental resolution and vertical calibration as in (a) and a quasistatic approximation to the cross section above T_c with the lowest-order expansion of the inverse static susceptibility, $\chi^{-1}(\vec{q}) = \chi^{-1}(0) + cq^2$, $c = 1.5 \times 10^5$ Å^2, and $\chi^{-1}(0)$ as given in Ref. 11.

When account is taken of the difference in incident neutron wavelength, resolution function, and averaging over polar scattering angle, one finds good agreement between the earlier Harwell and present ILL measurements for the small-angle scattering intensity over the q and temperature range where comparison can be made.

In the range $T_c \lesssim T \lesssim 50$ K the small-angle scattering intensity has been analyzed within the quasistatic approximation. In this approximation the differential cross section for diffuse spin scattering of unpolarized neutrons from a demagnetized specimen having a cubic lattice may be expressed in the form $\gamma T \chi(\vec{q})$, where γ is a constant and $\chi(\vec{q})$ is the static wave-vector–dependent susceptibility. Expanding the inverse of $\chi(\vec{q})$ to lowest order in $\vec{q}$ consistent with the cubic symmetry of the lattice we obtain $\chi^{-1}(\vec{q}) = \chi^{-1}(0) + cq^2 + \cdots$, where c is a coefficient related to that appearing in the usual Ginzburg-Landau expansion of the free-energy density as a power series in the gradient of the appropriate local magnetization.[10] As shown in

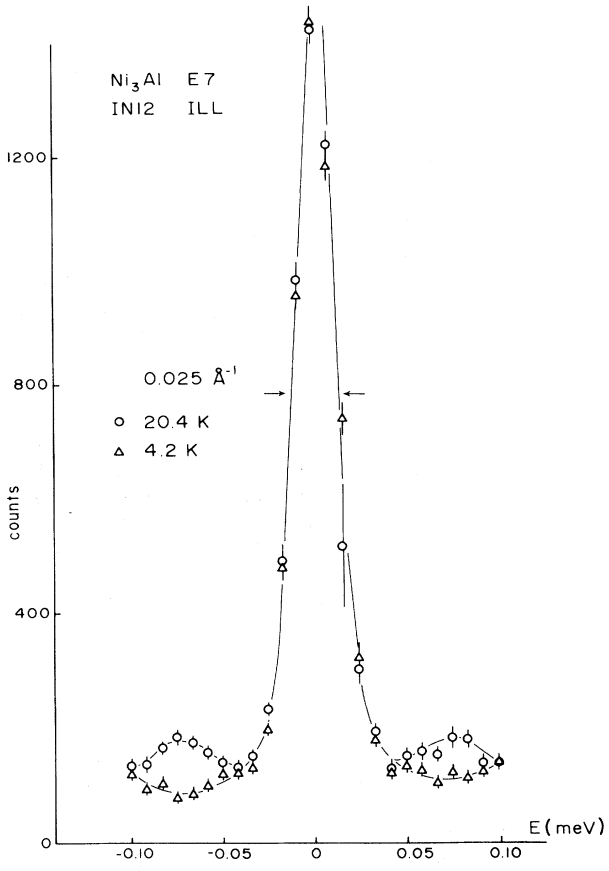

FIG. 3. Inealstic magnetic scattering from Ni_3Al as observed in the forward direction with the triple-axis crystal spectrometer IN12 at the ILL. The thermally induced scattered intensity lies in spin-wave peaks with no charge in the central elastic peak within experimental error. The width of the central elastic peak gives an indication of the typical experimental instrumental resolution (full width at half maximum $\simeq 0.025$ meV). The solid lines served to connect data points.

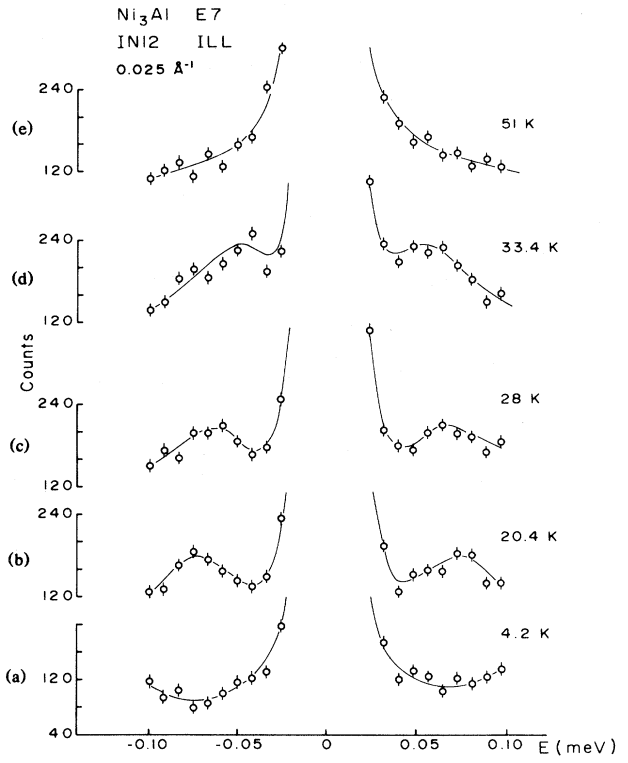

FIG. 4. Temperature dependence of inelastic magnetic scattering in Ni_3Al. Well-defined excitations, relative to 4.2-K background, up to temperatures $\simeq 33$ K, collapse in towards the elastic peak and become diffusive on raising the temperature and passing through T_c ($\simeq 41$ K). The solid lines serve to connect data points at a given temperature for constant scattering wave vector of 0.025 $Å^{-1}$.

Fig. 2(b) the approximate expression $\gamma T/[\chi^{-1}(0)+cq^2]$ for the cross section, when scaled by the measured calibration constant and convolved with the instrumental resolution function, is consistent with with the observed scattering intensity above T_c at least up to 50 K, given the assumption that $c=(1.5\pm0.3)\times10^5$ $Å^2$. The value of $\chi^{-1}(0)$ at each temperature was derived from bulk susceptibility measurements reported by de Boer.[11]

To confirm the spin-wave interpretation of the small-angle scattering cross section below T_c and to investigate the energy distribution of the scattering above T_c, energy-resolved studies were carried out on IN12 with a larger and purer sample, low background levels, and long counting times. The observed temperature dependence of the scattering intensity versus energy at a constant scattering wave vector of 0.025 $Å^{-1}$ is shown in Figs. 3 and 4. The variation of intensity with temperature can be attributed almost entirely to scattering from thermally excited modes which are propagating (i.e., have a well-defined energy) below T_c and are diffusive above T_c. No change is observed in the central elastic peak as a function of temperature below T_c. Measurements in the wave-vector range 0.020 to 0.035 $Å^{-1}$ at 20.4 K suggest that the excitation spectrum is approximately quadratic as expected for spin waves, with a stiffness of approximately 85 ± 15 meV $Å^2$, in good agreement with the value deduced from the small-angle scattering data. Possible information on the lifetimes and energy gap of the spin waves is masked by effects of instrumental resolution at small scattering angles.

In summary, the small-angle scattering and triple-axis measurements show that in the experimental wave-vector range the temperature dependence of the neutron scattering cross section can be well understood in terms of thermally excited spin waves below T_c. There is no evidence for the existence of other significant contributions to the temperature-dependent cross section as might be expected, for example, if magnetic heterogeneities due to structural disorder or impurities were important. The spin-wave peaks collapse to zero energy as T_c is approached. Near and above T_c we observe diffuse magnetic fluctuations whose characteristic correlation length $\lambda_c=[c\chi(0)]^{1/2}$ may be inferred from the small-angle scattering results and whose energy distribution can be estimated from the triple-axis measurements. To gain a more complete understanding of the precise role of magnetic excitations on the ground-state and thermal properties of Ni_3Al, further measurements at higher energies and momenta are required.

ACKNOWLEDGMENTS

We wish to thank Dr. B. D. Rainford and Dr. S. K. Burke for their valuable assistance in carrying out the small-angle scattering measurements.

[1]D. M. Edwards and E. P. Wohlfarth, Proc. R. Soc. London A303, 127 (1967).
[2]K. K. Murata and S. Doniach, Phys. Rev. Lett. 29, 285 (1972).
[3]T. Moriya and A. Kawabata, J. Phys. Soc. Jpn. 34, 639 (1973); 35, 669 (1973).
[4]T. Moriya, J. Magn. Magn. Mater. 14, 1 (1979).
[5]W. F. Brinkman and S. Engelsberg, Phys. Rev. 169, 417 (1968).
[6]D. Fay and J. Appel, Phys. Rev. B 22, 3173 (1980).
[7]N. R. Bernhoeft, I. Cole, G. G. Lonzarich, and G. L. Squires, J. Appl. Phys. 53, 8204 (1982).
[8]T. I. Sigfusson, N. R. Bernhoeft, and G. G. Lonzarich, J. Appl. Phys. 53, 8207 (1982).
[9]W. Marshall and S. W. Lovesey, *Theory of Thermal Neutron Scattering: The Use of Neutrons for the Investigation of Condensed Matter* (Oxford Univ. Press, Oxford, 1971) Chap. 9.3.
[10]C. Herring, in *Exchange Interactions Among Itinerant Electrons,* Magnetism: A Treatise on Modern Theory and Materials, Vol. 4, edited by G. T. Rado and H. Suhl (Academic, New York, 1966).
[11]F. R. de Boer, Ph.D thesis (University of Amsterdam, 1969) (unpublished).